

Substructures of martensite in Fe–1C–17Cr stainless steel

Hsin-Yi Lee, Hung-Wei Yen, Hsiao-Tzu Chang and Jer-Ren Yang*

Department of Materials Science and Engineering, National Taiwan University, Taipei, Taiwan, ROC

Received 17 December 2009; revised 12 January 2010; accepted 12 January 2010

Available online 15 January 2010

An Fe–1.0C–17Cr (wt.%) stainless steel was subjected to subzero treatment to investigate the structure of the martensite midrib. During the course of the isothermal holding in liquid nitrogen ($-196\text{ }^{\circ}\text{C}$), the thin-plate martensite formed first, and lenticular martensite later. The substructures of thin-plate martensites and lenticular martensite were examined using transmission electron microscopy, focusing on the details of the midrib. The results provide strong evidence to suggest that thin-plate martensite can be transformed into lenticular martensite.

© 2010 Acta Materialia Inc. Published by Elsevier Ltd. All rights reserved.

Keywords: Stainless steel; Martensitic phase transformation; Martensite midrib; Twinning; TEM

The morphologies and internal structures of martensites in Fe–Ni, Fe–Cr alloys have been intensively investigated by Wayman et al. [1–16]. In these alloy systems, there are primarily three different morphologies, namely lath, thin plate, and lenticular, depending on the alloy composition and martensite start (M_s) temperature. Lath martensite forms in the highest temperature range and contains a high density of dislocations. Thin-plate martensite, which forms in the high chemical composition alloys in the lowest temperature range, is composed of a set of uniformly spaced transformation twins crossing throughout the plate [8,9]. Lenticular martensite forms at an intermediate temperature between lath martensite and thin-plate martensite; it takes on a lens-like morphology and contains three regions: the midrib, extended twinned region and untwinned region [10–16]. The substructures of lenticular martensite are much more complicated than those of other types. In the optical metallographs, the midrib appears as a straight line dividing the lens-like structure in half, and giving it a symmetrical feature. Transmission electron microscopy has revealed that the midrib consists of highly dense and regularly spaced transformation twins. Although there are considerable reports on the martensite midrib [5–16], the detailed substructures and formation of the midrib have not been clarified yet. Shimizu et al. [5,8] studied Fe–Ni and Fe–Ni–Co alloys, and as-

serted that the midrib region had a different orientation from its surrounding extended twin region. On the other hand, Shibata et al. [15,16] investigated the thin-plate martensite in Fe–31Ni–10Co–3Ti (wt.%) alloy, which grew into a lenticular shape by 1% tensile deformation at a temperature slightly higher than its M_s temperature. The deformed thin-plate martensite had the substructures similar to the lenticular martensites in Fe–31Ni, Fe–33Ni and Fe–20.5Ni–35Co (wt.%) alloys. The effect of the deformation on thin-plate martensite caused the originally existing twins in the thin-plate martensite to be extended outwards to a range of about several hundred nanometers. From the result of a comparative elaboration, they claimed that the midrib in lenticular martensite was thin-plate martensite itself at the earliest stage formation of lenticular martensite. However, their explanation for the transition from thin-plate martensite to lenticular martensite is still debatable. Direct transmission electron microscopy (TEM) observation in the same alloy, without resorting to mechanical treatment, is required. Although there are several fundamental difficulties in assessing the substructures of lenticular martensite, such as sectioning and accommodation–distortion effects, TEM investigation continues to assume greater significance in research. In this work, it has been found that thin-plate and lenticular martensites co-existed in the specimens of AISI 440C stainless steel. This condition facilitated the efforts of TEM investigation.

The as-received material was a commercially wrought AISI 440C stainless steel bar (with a diameter of 122 mm) produced by Gloria Material Technology

* Corresponding author. Tel.: +886 2 23632756; fax: +886 2 23634562; e-mail: jryang@ntu.edu.tw

Corporation through four-folded forging of a cast slab at 1130 °C and annealing at 870 °C for 8 h, followed by furnace cooling to ambient temperature. The chemical composition of this steel was Fe–1.0C–17.4Cr–0.45Mo–0.40Mn–0.38Si (wt.%). The pieces of steel rod were machined from the half radius position of the original bar, and homogenized at 1200 °C for 3 days in quartz capsules containing pure argon, with subsequent quenching to room temperature. After the decarburization layer had been removed, an optical metallography (OM) sample was mechanically polished and etched in a mixture of 40 ml HCl, 25 ml ethanol, 30 ml distilled water and 5 g CuCl_2 . OM of the homogenized specimen was revealed to consist of austenite (92 vol.%) with small amounts of undissolved M_7C_3 carbide (8 vol.%). The M_s temperature was measured to be -48 °C via a TA differential scanning calorimetry (DSC) during the course of cooling at the rate of 10 °C min^{-1} (as shown in Fig. 1a). Thin-plate martensite was seen in the DSC sample cooled to -55 °C (as displayed in Fig. 1b), and lenticular martensite in the other DSC sample cooled to -150 °C (as presented in Fig. 1c). The results are not consistent with the general proposition that lenticular martensite forms at a higher temperature than the thin-plate martensite. In order to elucidate this controversial finding, the homogenized specimens were machined into 3 mm diameter cylindrical rods of 6 mm

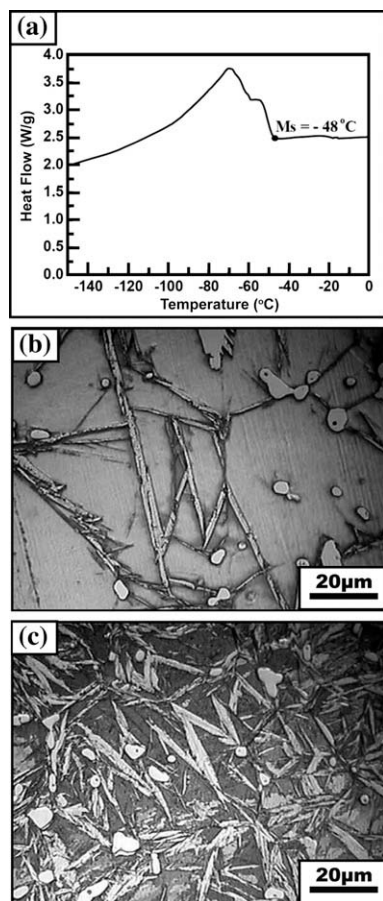


Figure 1. (a) DSC curve for determining M_s temperature of the homogenized sample, (b) OM taken from the DSC sample cooled to -55 °C, and (c) OM taken from the DSC sample cooled to -150 °C. (The lump-shaped particles: M_7C_3 .)

length for further investigation. The rod specimens were then subzero cooled by immersion into 1000 ml liquid nitrogen (-196 °C) in a vessel for different holding times (8 s, 10 s, 12 s and 30 min). The corresponding microstructures were examined using optical microscopy (OM) and TEM. TEM samples were sliced from the rod specimens, thinned to 0.08 mm by abrasion with SiC papers, and then twin-jet electropolished using a mixture of 5% perchloric acid, 25% glycerol and 70% ethanol at 5 – 10 °C with 35 – 40 V polishing potential. The thin foils were then examined using an FEI Tecnai G^2 20 TEM operated at 200 kV.

The series of optical metallographs presented in Figure 2a–d were obtained from the specimens subzero cooled at -196 °C for 8 s, 10 s, 12 s and 30 min, respectively. As can clearly be seen, the typical thin-plate martensite (as shown in Fig. 2a and b) forms at the earliest stage of the transformation, and the typical lenticular martensite (as shown in Fig. 2c and d) occurs after prolonged holding. It is notable that both lenticular and thin-plate martensites co-exist, as presented in Figure 2c and d. Thin-plate martensite has a morphology quite distinguishable from that of lenticular martensite. The thin-plate martensite exhibits a very narrow plate with a thickness of 1 – 3 μm and has an apparent aspect ratio (length/thickness) of 20/1 or greater. On the other hand, the lenticular martensite has smoothly curved interfaces and a larger thickness of 2 – 8 μm with a much smaller apparent aspect ratio (length/thickness) of 6/1.

Substructures of thin-plate martensite and lenticular martensite in the homogenized specimens subzero cooled at -196 °C for 30 min were investigated by TEM. Some representative features are displayed in Figures 3 and 4 and Supplementary materials. Figure 3a–d shows the substructures of a thin-plate martensite with a plate thickness of about 600 nm, in which a set of uniformly spaced highly dense internal transformation $\{112\}$ twins crosses throughout the plate. The morphology of the twinned substructure is highly dependent on the orientation of the thin foil. The zone axis $[113]_m // [1\bar{1}\bar{3}]_t$ was chosen as shown in Figure 3c and d, and the twin planes $(21\bar{1})$ exhibited an edge-on configuration to the incident elec-

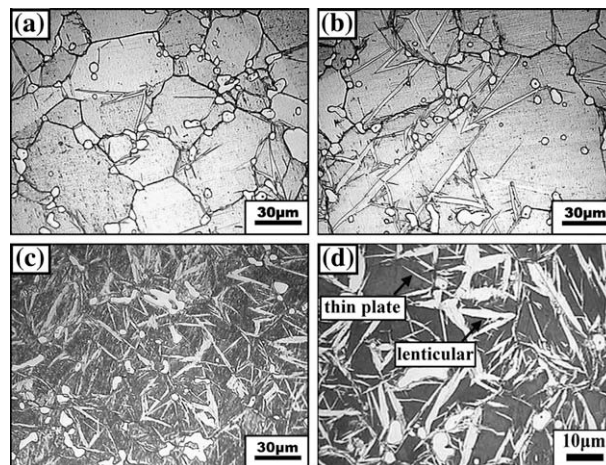


Figure 2. Optical metallographs taken from the homogenized specimens subzero cooled at -196 °C for (a) 8 s, (b) 10 s, (c) 12 s, and (d) 30 min. (The lump-shaped particles: M_7C_3 .)

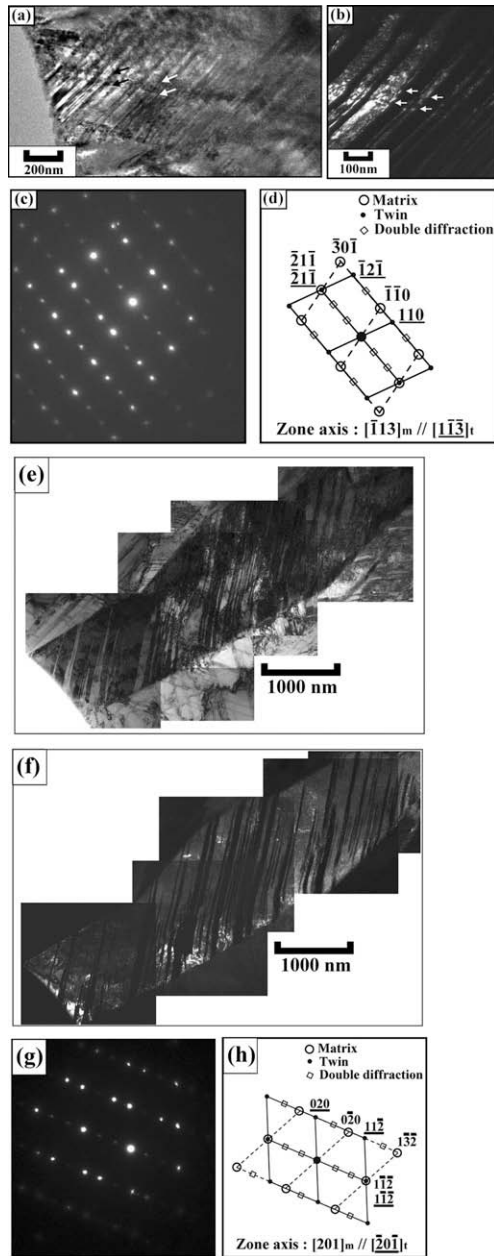


Figure 3. (a) A bright-field image of a thin-plate martensite, (b) a corresponding dark-field image illuminated by using $(1\ 1\ 0)_t$ reflection, (c) the selected area diffraction patterns (SADP), and (d) the corresponding analysis for (c); (e)–(h) showing another example of a thin plate martensite.

tron beam direction. Along the parallel twinning planes, the disconnected junctions can be identified as indicated by arrows in Figure 3a and b. Therefore, a narrow band about 60 nm in width along the center of the plate can be identified as the midrib. This result suggests that after the midrib is formed, there is a particular period of stasis growth in the earliest stage of the martensitic transformation. On the other hand, Figure 3e–h shows another example of TEM investigation of the thin-plate martensite; a set of $(1\ \bar{1}\ 2)$ transformation twins is not uniform in width, and no apparent midrib at the center region of the plate can be seen. It is noted that the twins are bent in the regions near both interfaces. The bending phenomenon is presumably due to the accommodation effect, and possi-

bly raises the difficulty in the observation of the midrib. A similar result has previously been reported for an Fe–1C–8Cr (wt.%) alloy [6].

Typical substructures of lenticular martensite are shown in Figure 4. The montages of TEM bright-field and dark-field images (Fig. 4a and b) reveal three sub-zones: the midrib, extended twinned region and untwinned region. It can be seen that the midrib (as shown in the area marked A in Fig. 4) has a width of about 100 nm running centrally along its axis. The extended twins give a lens-like feature; they emanate laterally from the midrib region and form a symmetrical pattern of parallel vertex pillars. The extension of twins is extremely rugged (as shown in the area marked B in Fig. 4). Some twins have grown laterally to a length greater than 1500 nm, but some twins are smaller than 300 nm. The thickness of the twins (ranging from 50 to 200 nm) also increased with the increase of the amount of extension. High-resolution transmission electron microscopy (HRTEM) was performed to investigate the junction between the midrib and the extended twin. In the low-magnification TEM in Figure 4c, the examined boundary is indicated by the marked rectangle. The corresponding HRTEM is presented in Figure 4d; the lattice image shows that the twin in the midrib has the same orientation as its neighboring extended twin. The TEM and HRTEM results provide strong evidence to suggest that the martensite transformation is initiated at the midrib region, and that the growth of lenticular martensite accompanies the extension of twins. That the extended twins cannot grow uniformly might possibly be due to the effect of the latent heat of transformation. In other words, the heat evolved from the twins which grew previously, interrupting the subsequent growth of adjacent twins starting from the midrib. The transformation heat is in an adiabatic way and should lead to a local temperature rise in lenticular martensite plate during growth. Since the overall transformation of lenticular martensite is diffusionless, the untwinned region is essentially associated with another lattice-invariant deformation mode, slip, which must involve the twinning elements, so that the perfect dislocations (acting as emissary dislocations) can slip along the twinning plane subsequently. The conservative movement of perfect dislocations plays a key important role in the formation of the untwinned region.

The untwinned region, as shown in the area marked C in Figure 4, can be seen to have some planar faults and dislocations. The defects associated with martensitic plate can be attributed to the fact that the shape deformation accompanying the martensitic transformation is accommodated by plastic relaxation. The resulting defects introduced into the austenite and the intrinsic stacking faults in the austenite can be inherited by the martensite that subsequently forms. Plastic relaxation may also follow in the martensite itself. The above effects bring about the complexity in the assessment of substructures. In this work, a particular TEM example shows that in a lenticular martensite plate two midribs co-exist and the secondary midrib branches off from the primary midrib (as seen in Supplementary materials). The possible mechanism can be considered as follows. At the initial stage, thin-plate martensite forms and another variant of thin plate joins together in a zigzag

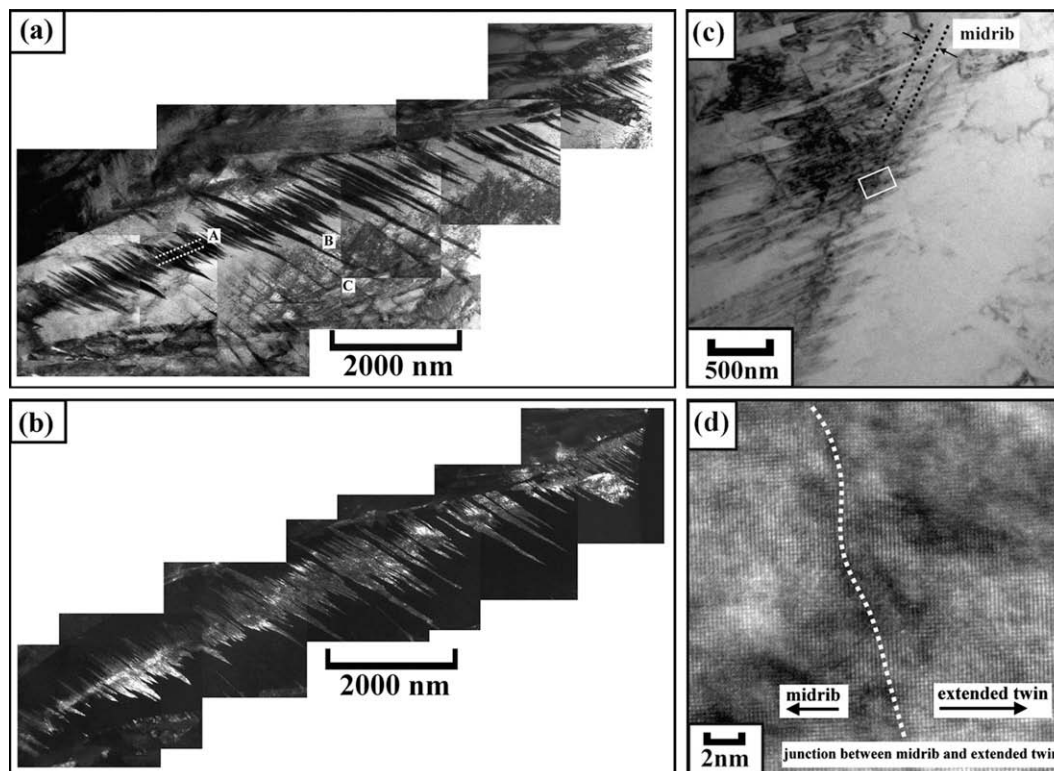


Figure 4. (a) A montage of TEM bright-field image of a lenticular martensite, (b) a montage of a corresponding TEM dark-field image, (c) a low-magnification TEM micrograph indicating the junction between midrib and its neighboring extended twin within the white marked rectangle, and (d) the corresponding HRTEM.

array. Afterwards, two thin plates transform to two lenticular plates and coalesce to form a larger lenticular plate. However, it should be noted that the TEM presents us with two-dimensional images of three-dimensional specimens, viewed in transmission. The interpretation of transmission images must be performed with caution because the superimposed structures are not discernible.

In summary, thin-plate martensite and lenticular martensite, which were found to co-exist in AISI 440C stainless steel, have been examined via DSC, OM, TEM and HRTEM. The results suggest that the transformations of thin-plate martensite and lenticular martensite are initiated at the same midrib region. During the growth, the former keeps the lattice-invariant deformation mode of twinning, whereas the latter combines both twinning and slip modes.

This work was carried out with the financial support from National Science Council of Republic of China, Taiwan, under Contract NSC 96-2628-E-002-015-MY2.

Supplementary data associated with this article can be found, in the online version, at [doi:10.1016/j.scriptamat.2010.01.022](https://doi.org/10.1016/j.scriptamat.2010.01.022).

- [1] K. Shimizu, M. Oka, C.M. Wayman, *Acta Metall.* 18 (1970) 1005.
- [2] S. Jana, C.M. Wayman, *Metall. Trans.* 1 (1970) 2825.
- [3] M. Watanabe, C.M. Wayman, *Metall. Trans.* 2 (1971) 2221.
- [4] B.P.J. Sandvik, C.M. Wayman, *Metall. Trans. A* 14 (1983) 2455.
- [5] R.L. Patterson, C.M. Wayman, *Acta Metall.* 14 (1966) 347.
- [6] K. Shimizu, M. Oka, C.M. Wayman, *Acta Metall.* 19 (1971) 1.
- [7] D.-Z. Yang, B.P.J. Sandvik, C.M. Wayman, *Metall. Trans. A* 15 (1984) 1555.
- [8] K. Shimizu, Z. Nishiyama, *Metall. Trans.* 3 (1972) 1055.
- [9] T. Maki, S. Shimooka, I. Tamura, *Metall. Trans.* 2 (1971) 2944.
- [10] R.P. Reed, *Acta Metall.* 15 (1967) 1287.
- [11] E.O. Fearon, M. Bevis, *Acta Metall.* 22 (1974) 991.
- [12] T. Kakeshita, K. Shimizu, T. Maki, I. Tamura, *Scripta Metall.* 14 (1980) 1067.
- [13] T.N. Durlu, *J. Mater. Sci. Lett.* 16 (1997) 1307.
- [14] A. Shibata, S. Morito, T. Furuhashi, T. Maki, *Scripta Mater.* 53 (2005) 597.
- [15] A. Shibata, T. Murakami, S. Morito, T. Furuhashi, T. Maki, *Mater. Trans.* 49 (2008) 1242.
- [16] A. Shibata, S. Morito, T. Furuhashi, T. Maki, *Acta Mater.* 57 (2009) 483.